Microbial lipid signatures and substrate potential of organic matter in permafrost deposits - implications for future greenhouse gas production

J.G. Stapel[1], L. Schirrmeister[2], P.P. Overduin[2], S. Wetterich[2], J. Strauss[2], B. Horsfield[1], and K. Mangelsdorf[1]

[1] GFZ, German Research Centre for Geoscience, Helmholtz Centre Potsdam, Organic Geochemistry, Telegrafenberg, 14473 Potsdam, Germany
[2] Alfred Wegener Institute, Helmholtz Centre for Polar and Marine Research, Research Unit Potsdam, Department of Periglacial Research, Telegrafenberg, A43, 14473 Potsdam, Germany

Corresponding author: Janina Stapel (Janina.Stapel@gfz-potsdam.de)

Key Points:

- Abundant microbial life in the active layer but living microorganisms are also identified in the permafrost deposits

- Increased past microbial activity is indicated in intervals of high OM accumulation with increased OM quality

- Future potential for greenhouse gas generation from permafrost deposits depend on the quality and amount of the OM

Index Terms:

- 0475 Permafrost, cryosphere and high-latitude processes

- 0428 Carbon cycle

- 0793 Biogeochemistry

- 1637 Regional climate change

Keywords:

- Phospholipids

- Phospholipid fatty acids

- GDGTs

- Carbon quality

- Arctic permafrost

- Greenhouse gas potential

Abstract

A terrestrial permafrost core from Buor Khaya in northern Siberia comprising deposits of Late Pleistocene to Early Holocene age has been investigated to characterize living and past microbial communities with respect to modern and paleoclimate environmental conditions, and to evaluate the potential of the organic matter (OM) for greenhouse gas generation. Microbial life markers - intact phospholipids and phospholipid fatty acids - are found throughout the entire core and indicate the presence of living microorganisms also in older permafrost deposits. Biomarkers for past microbial communities (branched and isoprenoid GDGT as well as archaeol) reveal links between increased past microbial activity and intervals of high OM accumulation accompanied by increased OM quality presumably caused by local periods of moister and warmer environmental conditions. Concentrations of acetate as an excellent substrate for methanogenesis are used to assess the OM quality with respect to microbial degradability for greenhouse gas production. For this purpose two acetate pools are determined: the pore-water acetate and OM bound acetate. Both depth profiles reveal similarities to the OM content and quality indicating a link between the amount of the stored OM and the potential to provide substrates for microbial greenhouse gas production. The data suggest that OM stored in the permafrost deposits is not much different in terms of OM quality than the fresh surface organic material. Considering the expected increase of permafrost thaw due to climate warming, this implies a potentially strong impact on greenhouse gas generation from permafrost areas in future with positive feedback on climate variation.

1 Introduction

Permafrost, defined as ground that remains at or below 0 °C for at least two consecutive years [*Washburn*, 1980], is a large reservoir for organic matter (OM) [*Christensen et al.*, 2004; *Hugelius et al.*, 2014] and a significant source of climate-relevant trace gases such as carbon dioxide (CO_2) and methane (CH_4) [*Wagner et al.*, 2003]. Generally, Arctic permafrost is of enormous importance for the global terrestrial carbon cycle [*Zimov et al.*, 2006] and is particularly vulnerable to future climate change [*Grosse et al.*, 2011]. Formation of permafrost in north eastern Siberia started in the Late Pliocene and persisted over the entire Pleistocene [*Arkhangelov et al.*, 1996]. During glacial periods permafrost deposits accumulated under continental, cold climate conditions [*Wetterich et al.*, 2011a] often accompanied by the growth of syngenetic ice wedges. Late Pleistocene ice- and particularly organic-rich permafrost deposits are known as Yedoma Ice Complex and are affected by alternating stadial/interstadial climate variations [*Strauss et al.*, 2012; *Schirrmeister et al.*, 2013; *Wetterich et al.*, 2014].

In response to the currently ongoing global climate change, an increase in ground temperature, a deepening of the active layer (seasonally thawed surface layer) and a spatial retreat of the extent of permafrost have already been reported at different sites in the Russian Arctic [*Anisimov*, 2007; *Romanovsky et al.*, 2010]. As a consequence, the freeze-locked OM becomes accessible to microbial degradation resulting in the formation and release of CO_2 and CH_4, which may cause a positive feedback on climate warming [*Knoblauch et al.*, 2013]. In the northern circumpolar permafrost terrain 999 Pg (1Pg = 1015 g = 1 Gt) of soil organic carbon is stored, of which 822 Pg is perennially frozen [*Hugelius et al.*, 2014]. The accumulation, preservation and distribution of the OM is strongly linked to a broad variety of paleo-environmental factors such as periglacial landscape dynamics, vegetation, paleo-relief and climate forcing [*Schirrmeister et al.*, 2011]. The surface OM in the active layer derived

from current vegetation in the tundra and is mainly composed of mosses, lichens, grasses, sedges and dwarf shrubs. On the other hand, the OM stored in the permafrost originates from fossil plant remains and is poorly degraded [*Knoblauch et al.,* 2013]. Therefore, the OM within permafrost can form an important source of substrates for microbial degradation processes and finally the release of greenhouse gases. Due to large scale thawing and subsequent increasing microbial activity, the permafrost deposits can turn from a carbon sink into a source [*Schuur et al.,* 2009].

Low molecular weight organic acids (LMWOA) such as acetate are important and easily convertible substrates for microbial metabolism [*Sørensen et al.,* 1981; *Ganzert et al.,* 2007; *Vieth et al.,* 2008] and are, therefore, used as a quality indicator in terms of future microbial degradability of the sedimentary OM [*Glombitza et al.,* 2009; *Strauss et al.,* 2015]. LMWOAs can either be dissolved in pore water and cryostructures (pore ice, segregated ice) of permafrost deposits as free substrates being directly bioavailable for microorganisms (e.g. methanogens, acetogenic bacteria and sulfate reducers) or they can be bound to the complex organic matrix (e.g by ester-linkage) forming a future substrate pool after liberation due to geochemical or microbial alteration of the OM [*Glombitza et al.,* 2009].

In addition to microbiological studies, the microbial community can be investigated by the analysis of microbial molecular markers (biomarkers) such as phospholipids (PLs) and phospholipid fatty acids (PLFAs), which are essential membrane components of living cells [*Zelles,* 1999]. In general, PLs are hydrolysed rapidly after cell death [*White et al.,* 1979] and therefore they represent good indicators for the presence of viable microorganisms in sediments [*Haack et al.,* 1994; *Rütters et al.,* 2002a]. Additionally, analysis of intact PLs, especially their fatty acid (FA) side chain inventory (PLFA), enables to identify and distinguish between different groups of microorganisms contributing to the microbial community [*Rütters et al.,* 2002b]. Therefore, PLs are considered to be suitable life markers for microbial communities [*White et al.,* 1979; *Zink et al.,* 2003]. Glycerol dialkyl glycerol tetraether (GDGT) lipids are membrane compounds synthesized by archaea (isoprenoid alkyl-chains) [*Koga,* 1993; *Pancost et al.,* 2001; *Koga and Morii,* 2006] and bacteria (branched alkyl-chains) [*Weijer et al.,* 2006a*; Schouten et al.,* 2013]. Additionally, the glycerol phytanyl diether archaeol is widespread in archaea [*Lim et al.,* 2012]. In contrast to the PL life markers, GDGTs and archaeol represent membrane lipids of past microbial biomass, since they are already partly degraded as indicated by the loss of their head groups. The remaining core lipids are less affected by degradation processes and are, therefore, stable over geological time scales [*Pease et al.,* 1998].

With the progression of permafrost thawing and the associated increase of available OM, the question on the quality of the OM with regard to microbial biodegradability and greenhouse gas production arises. Therefore, the aim of this paper is to study the role of the microbial community in the transformation of the OM from the active layer to the underlying permafrost sequence with specific regard to future climate relevant greenhouse gas production. We focus on the relationship between the past and present microbial communities, the availability of substrates, and the OM characteristics (quality, quantity, and stored potential) to estimate how Late Glacial/Early Holocene and Late Pleistocene permafrost deposits can be affected by microbial transformation and how the system might respond to future climate warming.

2 Study area and material

The Buor Khaya Peninsula is located in the Sakha Republic (Yakutia) in north-eastern Siberia, Russia (Fig. 1a,b). It is underlain by continuous permafrost with an estimated thickness of 450 to 650 m [*Romanovskii et al.,* 2004] and ground temperatures of less than -11 °C [*Drozdov et al.,* 2005]. The region is part of western Beringia, a landmass that was mostly non-glaciated during the Late Pleistocene and which stretched from the Eurasian Ice Sheet in the west to the Laurentide Ice Sheet in the east [*Hopkins,* 1998]. The Buor Khaya Peninsula is dominated by ice-wedge polygonal tundra. The relief includes ice-rich Yedoma uplands and drained thermokarst basins (land-surface configurations that result mainly from ground ice melt in permafrost regions) [*Strauss et al.,* 2015]. The coldest mean monthly air temperature in the study area of -36 °C is measured in January while a mean temperature of 10 °C is measured during the warmest months July and August. Most precipitation occurs between June and September as well as in December [*Wetterich et al.,* 2011b]. The active layer thickness is estimated between 20 to 40 cm [*Günther et al.,* 2015]. The field work for this study was conducted during a drilling campaign undertaken by the Alfred-Wegner-Institute for Polar and Marine Research in April 2012. A 18.9 m long terrestrial permafrost core was drilled in approximately 200 m distance from the coast on top of a Yedoma hill (71°25′13"N, 132°06′38"E; Fig. 1c) using a rotary drill rig (KMB, rotary) [*Günther et al.,* 2013]. The core consists of silty sediments with visible organic remains and exhibits different kinds of cryostructures such as horizontal, vertical and reticulated ice, lenses and ice-cement (Fig. 2). Additionally, the core contains an ice wedge spanning from ca. 3.2 to 8.7 m depth, separating Late Glacial/Early Holocene from deeper Late Pleistocene Yedoma deposits [*Schirrmeister et al.,* 2016]. The sedimentary part below the ice wedge is characterized by nearly vertical ice layers from 8.7 to 10.6 m, indicating tilting of the sediment deposits due to syngenetic ice-wedge growth. From 10.6 m down to about 16 m core depth horizontal ice layers dominate, and below ca. 16 m a diminished occurrence of cryostructures combined with coarse-grained sandy material was recognized. The drilled core segments were kept frozen after coring and were transported in a frozen state for further processing to Potsdam, Germany. In the home laboratory sampling was conducted in a cold storage at -10 °C. A total of 20 inner core samples were taken. With the exception of the ice wedge, samples were taken at intervals of 30-120 cm throughout the entire core. Finally, samples were investigated for microbial biomarkers, pore-water composition, free and bound acetate concentrations as well as OM characteristics such as total organic carbon (TOC) content, stable carbon isotope ratio (δ^{13}Corg), TOC/TN ratio (TN = total nitrogen), hydrogen (HI) and oxygen (OI) indices, and open-system pyrolysis products (described below).

3 Methods

3.1 Sediment parameters

After freeze-drying and grinding of the permafrost samples, the TOC (wt%) and TN (wt%) content, and the δ^{13}Corg (‰) ratio of the bulk OM were determined. For TOC analysis sample material was treated with diluted HCl (HCl:water 1:9) at 60 °C to remove the inorganic carbon and measured on a LECO SC-632. To obtain further information on the basic characteristics of the OM the HI and OI were determined by Rock-Eval pyrolysis using a Rock-Eval 6 instrument. Measurements on the OM characteristics were conducted by Applied Petroleum Technology AS (Kjeller, Norway). To determine TN, samples were measured by a carbon-nitrogen-sulphur analyzer (Vario EL III, Elementar) with a device-specific accuracy of ± 0.1 wt%. For bulk δ^{13}Corg analysis, 1 mg sediment was placed in silver capsules, treated with 20 % HCl at 75 °C for carbonate removal, and subsequently

processed in a Carlo Erba NC 2500 elemental analyzer coupled to a Finnigan DELTA plus XL isotope mass spectrometer. By repeating control measurements, correct analytical values of better than ± 0.15 ‰ compared against the Vienna-Pee Dee Belemnite (VPDB) standard were ensured. To obtain additional information on the characteristics of the macromolecular structure of the OM a non-isothermal open-system pyrolysis was utilized after *Horsfield et al.* [1989]. Measurements were conducted on a pyrolysis-gas chromatograph (AGILENT GC 6890A Chromatograph) equipped with a flame ionization detector (Py-GC-FID). Five freeze-dried and grinded 10 mg samples including the active layer and four permafrost samples of different organic carbon content were analyzed.

3.2 Pore-water analysis

For the measurement of dissolved LMWOAs (acetate as a substrate) and anions (nitrate and sulfate as potential electron acceptors) within the pore water and ice, about 15 to 45 g (depending on the ice content) of the still frozen sample were transferred into a centrifuge tube with an internal filter inset, allowing separation of the pore water from the sediment in the centrifuge tube. The sample was placed in a refrigerator at 4 °C and slowly thawed over 12 h. Subsequently, the water was removed from the sediment by centrifugation (Sigma, laboratory centrifuge 6K15, 2500 rpm (908 x g), 20 °C, 10 min) and analyzed twice by ion chromatography with conductivity detection (ICS 3000, Dionex). Blanks contained negligible amounts of LMWOAs from filter material. Details of the pore-water analysis are described in *Strauss et al.* [2015].

3.3 Microbial lipid biomarker analysis

Approximately 50 g of the freeze-dried and grounded sample were extracted by using a flow blending system with a 200 ml mixture of methanol/dichloromethane/ammonium acetate buffer (2:1:0.8, pH 7.6) modified after *Bligh and Dyer* [1959].

The solvent extract was transferred into a separation funnel for phase separation. As internal standards, 50 µg of 1-myristyl-(D27)-2-hydroxy-sn-glycerol-3-phosphocholine, 10 µg of 5-α-androstane-17-one, 5-α-androstane, erucic acid (docosa-13-enoic-acid) and 1-ethylpyren were added. For phase separation dichloromethane and water were added to achieve a ratio of 1:1:0.9 of methanol/dichloromethane/ammonium acetate buffer mixture and the organic phase was removed. The water phase was re-extracted two times with dichloromethane and all organic phases were combined. Subsequently, the obtained sediment extract was separated into four fractions of different polarity (low polar lipids, free FAs, glycolipids, and PLs). Two columns were used in sequence. The upper column was filled with 1 g silica gel (63 - 200 µm) and topped with 0.5 g of sodium sulfate. The lower column was filled with 1 g - Florisil®. According to the method described by *Zink and Mangelsdorf* [2004], the low polar fraction was eluted with 20 ml of chloroform, the free FAs with 50 ml of methyl formiate blended with 12.5 µl of glacial acetic acid and the glycolipid fraction with 20 ml of acetone. After removal of the Florisil® column the PLs were eluted with 25 ml of methanol from the silica column. To improve the recovery of PLs, the silica column was rinsed with 25 ml of a methanol/water mixture (60:40) and the extract was captured in a separation funnel. 15 ml of dichloromethane and 3.5 ml of water were added for phase separation (methanol/dichloromethane/water, 1:1:0.9), the organic phase was removed, and the water phase was re-extracted two times with dichloromethane. Finally, the organic phases were combined and all fractions were evaporated to dryness and stored at - 20 °C until analysis.

3.3.1 Detection of Phospholipid Fatty Acids (PLFA)

After sediment extraction and column separation, one half of the PL fraction was used for PLFA analysis following a FA cleavage procedures described in *Müller et al.* [1998]. Subsequently, the resulting PLFAs were measured by gas chromatography-mass spectrometry (GC-MS). The GC-MS measurements were conducted on a Trace GC Ultra (Thermo Electron Corporation) coupled to a DSQ Thermo Finnigan Quadrupole MS (Thermo Electron Corporation). The GC was equipped with a cold injection system operating in the splitless mode and a SGE BPX 5 fused-silica capillary column (50 m length, 0.22 mm ID, 0.25 µm film thickness) using the following temperature conditions: initial temperature 50 °C (1 min isothermal), heating rate 3 °C/min to 310 °C, held isothermal for 30 min. Helium was used as carrier gas with a constant flow of 1 ml/min. The injector temperature was programmed from 50 to 300 °C at a rate of 10 °C/s. The MS operated in the electron impact mode at 70 eV. Full-scan mass spectra were recorded from m/z 50 - 650 at a scan rate of 1.5 scans/s. Blanks did not contain any PLFA.

3.3.2 Detection of Intact Polar Lipids (IPL)

The other half of the PL fraction was analyzed for IPLs using high performance liquid chromatography-mass spectrometry (HPLC-MS). The analyses were performed on a Shimadzu LC10AD HPLC instrument coupled to a Finnigan TSQ 7000 triple quadrupole MS with an electrospray ionization (ESI) interface. Samples were chromatographically separated on a LiChrospher 100 diol column (2 x 125 mm, 5 µm; CS-Chromatography Service) equipped with a pre-column filter. The mobile phase consisted of eluent A, a mixture of *n*-hexane/isopropanol/formic acid/ammonia (79:20:1.2:0.04 v/v; 25 % in water), and eluent B, a mixture of isopropanol/water/formic acid/ammonia (88:10:1.2:0.04 v/v, 25 % in water). Compound separation was achieved by the following solvent gradient: 1 min 100 % A, changed over 20 min to 35 % A and 65 % B using a linear gradient followed by 40 min of reconditioning. The flow rate was set to 0.35 ml/min. The ESI conditions were as followed: spray voltage 4; capillary temperature 220 °C; nitrogen sheath gas at 60 psi; without auxiliary gas. Mass spectra were generated in the negative ion mode over the range m/z 460 - 1100 at a scan time of 2 s. The injection was performed by an autosampler (HTC PAL, CTC Analytics). The individual PL concentrations are an average of triplicate measurements with a relative standard deviation of 0.01 to 0.17 %. Blanks did not contain any PLs.

3.3.3 Detection of Glycerol Dialkyl Glycerol Tetraethers (GDGT) and archaeol

After sediment extraction and column separation, the low polar lipid fraction was dissolved in 250 µl dichloromethane/methanol (99:1) and a 40-fold excess of n-hexane (10 ml) was added to precipitate asphaltenes. Asphaltenes were separated from the soluble extract by filtration over sodium sulfate. The *n*-hexane soluble fraction was subsequently separated into an aliphatic/ alicyclic and an aromatic hydrocarbon fraction, as well as into a polar fraction containing nitrogen, sulphur, and oxygen (NSO) bearing compounds using a medium-pressure liquid chromatography (MPLC) [*Radke et al.,* 1980].

An aliquot of the NSO fraction was investigated for tetraether lipids using a Shimadzu LC20AD HPLC instrument coupled to a Finnigan TSQ 7000 triple quadrupole MS with an atmospheric pressure chemical ionization (APCI) interface. Samples were chromatographically separated by using a Prevail Cyano column (2.1 x 150 mm, 3 µm; Alltech) equipped with a pre-column filter following a method described by *Schouten et al.* [2007]. The mobile phase consisted of an *n*-hexane A and isopropanol B (5 min, 99 % A, 1 % B) linear gradient: 1.8 % B with 40 min, in 1 min to 10 % B, held for 5 min to clean the column and back to initial conditions in 1 min, held for 16 min for equilibration. The flow

rate was set to 200 μl/min, and the injection was performed by an autosampler (HTC PAL, CTC Analytics). The APCI conditions were as follows: corona current 5 μA, giving a voltage of around 5 kV; vaporizer temperature 350 °C; capillary temperature 200 °C; nitrogen sheath gas at 60 psi; without auxiliary gas. Mass spectra were generated by selected ion monitoring in the positive ion mode at a scan rate of 0.33 s. The individual GDGT concentrations are an average of triplicate measurements with a relative standard deviation of 0.07 to 0.15 %. Blanks did not contain any GDGTs.

3.4 Alkaline cleavage reaction

To detect LMWOAs bound to the complex OM an alkaline cleavage approach was conducted as developed by *Glombitza et al.* [2009]. After sediment extraction, 5 g of the sediment was additionally pre-extracted with methanol to ensure that the compounds obtained after alkaline hydrolysis indeed represent the ester-bound fraction. The sediment was dissolved in 50 ml 1 N KOH solution in methanol and refluxed for 5 h. 50 μg 5-α-androstan-17-one and 50 μg erucic acid (docosa-13-enoic-acid) were added as internal standards after the suspension was cooled to room temperature. The suspension was filtered and the filter cake was thoroughly washed with methanol. Finally, methanol was evaporated from the alkaline cleavage solution under reduced pressure in a rotary evaporator (Büchi Rotavapor R205) leading to the precipitation of the corresponding potassium salts of the liberated FAs. The potassium salts were dissolved in water and the solution was adjusted to pH 8-10 with an aqueous solution of 5 % HCL. Afterwards, the alkaline solution was transferred into a 20 ml volumetric flask and topped up with water. Finally, this solution was used for ion chromatographic analysis of the formerly bound LMWOAs.

4 Results

According to difference in cryostructures, lithologies and age (radiocarbon dating by *Schirrmeister et al,* [2016]), the core was subdivided into three intervals. Interval I, from the ground surface down to 3.2 m, consists of fine sediments with visible organic root fragments and different types of cryostructures as described by *Schirrmeister et al.* [2016] (Fig. 2). This interval includes the active layer and is of Late Glacial/Early Holocene age (11.4 to 9.7 ka BP). Interval II, from 3.2 to 8.7 m, is characterized by an ice wedge that presumably formed during the Last Glacial Maximum (22.1 to 16 ka BP). Interval III (> 49 ka PB) comprises the sedimentary succession below the ice wedge from 8.7 to 18.9 m and is composed of silty sediments with visible organic remains and fine lens-like cryostructures which are typical for Late Pleistocene Yedoma deposits [*Schirrmeister et al.,* 2011].

4.1 Qualitative and quantitative analysis of the organic matter

Basic OM parameters, TOC, HI and TOC/TN (Fig. 3a-c), correlated throughout the entire core, although the variations in the TOC/TN ratio were less pronounced. TOC was of its highest (5.6 wt%) in the active layer and decreased in the underlying permafrost sequence. Interval I between 2 and 2.8 m was characterized by values of 2.5 to 4.5 wt%. In interval III the lowest TOC content of 0.9 wt% at 11.2 m was measured below the ice wedge, followed by a section of higher TOC contents (2.1 to 3.8 wt%) between 11.2 and 15 m, and by low values of 1.3 wt% at the end of the core. A similar depth trend was visible for the HI profile (R^2=0.40, p=0.006) with values between 331 and 104 mg HC/g TOC, and for the TOC/TN profile (R^2=0.46, p=0.001) varying between 12.25 and 8.55. Compared to the TOC, the increase at 10 m was much more pronounced in the HI profile. The OI profile (Fig. 3d) showed an inverse trend compared to the HI profile. In interval I, OI values increased with depth towards 195 mg CO_2/g TOC. In interval III the OI indicated its minimum at 10 m (165

mg CO_2/g TOC) and its highest values at 11.2 (232 mg CO_2/g TOC), 12.6 (231 mg CO_2/g TOC) and 16.8 m (249 mg CO_2/g TOC).

The δ^{13}C profile (Fig. 3e) showed an overall increasing trend with depth. While in interval I the values increased from -27.7 to -26.6 ‰, in interval III they showed stronger variability within the overall increasing trend. The profile showed negative excursions at 10 (-28.1 ‰) and 14.1 m (-27.2 ‰) and a positive shift at 12.6 m (-25.3 ‰).

A deeper insight into the OM quality was provided by pyrolysis experiments of five selected samples (high/low TOC and HI) (Fig. 4). All samples showed a relatively high phenol content and plotted into the range of kerogen type III representing terrestrial OM (Fig. 4a). Figure 4b indicates different aliphatic compositions of the selected samples. Generally, the data indicated an increasing aliphatic character of the OM with increasing TOC and HI. The sample from 10 m depth also showed a high aliphatic character despite of a relatively low TOC content. However, this sample revealed the highest HI, indicating OM with a comparatively high proportion of aliphatic structural moieties. All samples showed a very low abundance of sulphur compounds (data not shown) indicating sulphur lean OM.

The free acetate concentration varied between 6 to 475 mg/l in the permafrost deposits (Fig. 3f). In interval I the acetate profile was low even in the active layer with only a small rise in concentration above the ice wedge. In interval III the profile showed a similar trend to TOC with a minor increase in concentration at 10 m (169 mg/l) and higher concentrations between 12 and 15 m (196 to 475 mg/l). In contrast to the free acetate, the bound acetate concentration was high (65 mg/l) in the active layer (Fig. 3g). In interval I the concentration varied between 21.8 and 68.4 mg/l, while in interval III increased concentrations of 25 to 74 mg/l were measured between 11.2 and 15 m. Overall, the bound acetate profile resembled the TOC curve, especially in interval III (R^2=0.8; p=0.008).

Almost no sulfate (Fig. 3h) was measured within interval I. Below the ice wedge, intermediate concentrations of 25 to 80 mg/l were observed between 9 to 11.2 m. However, below 16 m sulfate concentrations were much higher (150 to 467 mg/l). Nitrate (Fig. 3i) varied between 0.2 and 3.5 mg/l. The active layer sample showed only low concentration of nitrate (0.5 mg/l), whereas in interval I and III higher nitrate concentrations at 2, 2.8, 10 m and between 12 and 15 m were detected.

4.2 Qualitative and quantitative analysis of microbial phospholipids

The microbial membrane phospholipid (PL) signature consisted mainly of phosphatidylethanolamine (PE), -choline (PC) and -glycerol (PG) esters, whereas the PEs are the dominant PL class representing more than 50 % of the identified PL and, therefore, mainly determined the total PL profile. However, the PL fraction contained a series of other signals which could not be identified yet, and therefore, only the identified peaks were incorporated into the total PL concentration. The highest abundance of PLs (Fig. 5a) was detected in the active layer with 33.3 µg/g sediment. In the permafrost sequence, the overall PL concentration was lower with values ≤ 4.4 µg/g sediment in interval I. In the upper part of interval III the PL concentration decreased to 2.1 µg/g sediment, but increased towards 5 µg/g sediment at 11.2 m. Between 11.2 and approximately 15 m, the PL concentrations were constantly higher with values between 3 to 4 µg/g sediment. Below 15 m, the PL concentration decreased to 0.9 µg/g sediment.

As expected, PLFA variability (Fig. 5b) was similar to the PL curve (R^2=0.95). A strong decrease in PLFAs from the active layer sample (97 µg/g sediment) into the permafrost sequence (2.7 µg/g sediment at 1.5 m) was observed. Furthermore, an increase in PLFA concentrations was also visible directly above the ice wedge and in the sequence

between 11.2 and 15 m. It can be noted that the PL concentration is lower than the PLFA concentration. Reasons for this are that only the main identified phospholipids (PEs, PGs and PCs) are incorporated into the total PL signal, and that PLs and PLFAs are measured and quantified on different analytical systems (HPLC-MS vs. GC-MS). Although the quantified data are consistent within the PL or PLFA profile, both mentioned reasons complicate a direct comparison of the quantified data. Thus, for a quantitative assessment of the microbial community the PLFA data are more reliable. However, more important than the concentration is that both profiles show similar trends indicating a link between both parameters. Therefore, both the PL and PLFA profiles dependably indicate depth variations of a viable microbial community.

The *iso-* to *anteiso*-FA ratio (Fig. 5c) showed constant values of about 0.64±0.04 throughout the permafrost sequence. Only the two uppermost samples (0.53 and 0.73) and the sample from 11.2 m (0.51) deviated. Almost the same was observed in the saturated- to unsaturated- FA ratio (Fig. 5d). The active layer showed higher relative amounts of *anteiso-* and unsaturated FA (0.56) compared to the permafrost sequence (0.72±0.06).

4.3 Qualitative and quantitative analysis of past microbial biomarkers

Branched and isoprenoid GDGTs as well as archaeol were detected in the entire permafrost core (Fig. 5e-g). The branched GDGTs (br-GDGTs) comprised mainly of GDGT-I, GDGT-Ib, GDGT-II and GDGT-III and were present at all depths (Table S1, supporting information). The highest concentration of br-GDGTs was detected in the active layer (3292 ng/g sediment) and much lower concentrations were measured in the permafrost sequence (down to 135 ng/g sediment). As observed for the PLs, concentrations were increased in interval I above the ice wedge (551 ng/g sediment). In interval III higher concentrations were found at 10 m and between 11.2 to 15 m, both of which fitted with maxima in TOC and HI (Fig. 3a,b).

Archaeol and glycerol dibiphytanyl glycerol tetraether (GDGT-0; Table S1; Fig. 5f-g) were most abundant in the active layer (264 ng/g sediment and 10 ng/g sediment, respectively) and much lower in the permafrost sequence. In contrast to the br-GDGTs, the variation and concentration of both were comparatively low within the deeper part of interval I. In interval III both profiles showed higher concentrations at 10 and around 14 m. At the bottom of the core, almost no br-GDGTs or archaeol were detected.

The ratio of archaeol to crenarchaeol (Fig. 6h) was close to 1 within interval I and the upper part of interval III. Below 11.2 m variations of the ratio correlated with the br-GDGT, GDGT-0 and archaeol. At the end of the core (below 16 m) the ratio decreased. The branched and isoprenoid tetraether (BIT) index was calculated after *Hopmans et al.* [2004]:

$$BIT\ index = \frac{([I]+[II]+[III])}{([I]+[II]+[III]+[crenarchaeol])}$$

The BIT index observed here was 1 or close to 1. Only at the bottom of the core a small decrease to 0.81 was observed (Table S1).

5 Discussion

5.1 Biomarkers for living microbial communities in permafrost deposits

Evidences for living bacteria are given throughout the entire core by the occurrence of PLs and PLFAs. However, their applicability as biomarker for currently living microorganisms in permafrost is more limited relative to unfrozen soils, but they likely represent a current and recently living microbial community. Since living microorganisms have already been detected in permafrost systems [*Gilichinsky and Wagener*, 1995; *Rivkina et al.,* 2004], the PL and PLFA signals are used as life makers in this study.

In active layers microbial life is generally more increased compared to permafrost deposits [*Kobabe et al.,* 2004; *Steven, et al.* 2006; *Wagner,* 2007]. Also in this study an abundant microbial life is indicated in the active layer by the intense PL life marker signal (Fig. 5a,b) and substantial microbial activity is reflected by relative low concentrations of the freely available substrate acetate, being an excellent substrate for microbial metabolism [*Ganzert et al.,* 2007]. Thus, the data indicate that the active layer hosts an increased and active microbial community and contains OM allowing intensified microbial turnover during the unfrozen state [*Zimov et al.,* 2006; *Lee et al.,* 2012; *Knoblauch et al.,* 2013].

In contrast, in the permafrost deposits the strongly decreased amount of life markers indicates lower abundance of microbial life and the comparatively high pore-water concentration of acetate in sections with increased TOC bears evidences for a very low microbial activity, since high microbial activity would have significantly reduced the free acetate concentrations. Living microorganisms in the permafrost deposits are most likely remnants or successors of the microbial community incorporated into the sediments during time of deposition [*Bischoff et al.,* 2013]. Generally, the PL profile in the permafrost sequence reveals that higher life marker abundances are linked to intervals of increased OM accumulation indicating a coupling of the permafrost microbial communities to the buried OM.

The PLFA inventory (Fig. 5c,d) of the bacterial community suggests that the community is composed of different bacterial groups regulating the cell membrane temperature adaptation to the cold ambient temperature conditions either via the ratio between *iso-* and *anteiso*-FAs or via the ratio between saturated and unsaturated FAs. According to *Rilfords et al.* [1978], most microorganisms alter their membrane composition and structure to bring the solid-liquid transfer temperature of the cell membranes below the ambient temperature and, therefore, maintain the membrane fluidity [*Russell,* 1989]. Higher proportions of *anteiso* and unsaturated FAs indicate adaptation to colder conditions. Both the *iso/anteiso and* saturated/unsaturated FA ratio are relatively constant within the permafrost sequence, which seem to resemble the permanently negative temperature conditions in the permafrost deposits with mean values of about -10 °C [*Schirrmeister et al.,* 2016]. In the active layer slightly lower ratios might reflect strong annual temperature variations and harsh winter conditions with lower temperatures than in the underlying permafrost deposits [*Wagner et al.,* 2005].

5.2 Biomarkers as indicators for past microbial communities and past environmental conditions in permafrost deposits

In the active layer the increased concentrations of GDGTs and archaeol most likely reflect remains deriving from the actually living and active microbial community consistent with the strong increase of life markers. In contrast, in the permafrost deposits with low life-marker signals the detected GDGTs and archaeol mainly represent the past bacterial (br-GDGTs, [*Weijers et al.,* 2006b]) and archaeal (iso-GDGTs and archaeol, [*Koga et al.,* 1993; *Pancost et al.,* 2001]) biomass influenced by past environmental conditions.

The br-GDGT-I, -II and -III are found in all core samples and reported to be the most abundant type of GDGTs in soils [*Weijers et al.,* 2006b]. Therefore, an increased past terrestrial bacterial community is indicated by higher concentrations of br-GDGTs in the permafrost deposits of interval I (above the ice wedge) and interval III between 10 and 15 m corresponding to higher TOC and HI values and a more aliphatic character of the OM. Generally, a positive correlation of TOC and HI indicates variations of TOC accompanied by changes in OM composition and quality [*Wilkes et al.,* 1999]. Higher HI values usually indicate a high proportion of hydrogen-rich OM, which is based on the amount of aliphatic hydrocarbons generated through thermal cracking from the complex OM. A higher aliphatic in contrast to aromatic character is suggested to resemble a better quality of OM with respect to its degradation and for greenhouse gas generating microorganisms [*Schön,* 1999; *Peters et al*., 2005]. Therefore, in addition to HI as a parameter for different OM sources, HI can be used as in indicator for OM quality [*Talbot and Livingstone,* 1989]. Data in the current paper show that high HI values seem to correspond to a higher aliphatic character of the OM indicating an increased OM quality in terms of microbial degradability (Fig. 3b and 4b). Based on that, we suggest that the amount and quality of OM is responsible for the increased past bacterial abundance in the Late Pleistocene.

Archaeol has been postulated as a proxy for the biomass of methanogens [*Pancost and Sinninghe Damsté,* 2003]. Thus, it can be used as a proxy for CH_4 production within terrestrial soils [*Lim et al.,* 2012] and to reconstruct changes in the abundance of methanogenic archaea in permafrost systems [*Pancost et al.,* 2011; *Bischoff et al.,* 2013]. GDGT-0 (Fig. 5g, Table S1) is the most common iso-GDGT in archaea and occurs in nearly all major groups of archaea [*Schouten et al.,* 2013]. It is often linked to methanogenic Euryarchaeota [*Koga et al.,* 1993] and is predominantly found in wetland environments [*Pancost et al.*, 2000]. Therefore, relatively high concentrations of archaeol and GDGT-0 indicate abundant presence of methanogenic archaea in the active layer but also in the permafrost deposits between 10 and 15 m and correspond to increased TOC, HI and pore-water acetate concentrations (Fig. 3 and 5f,g). Interestingly, the maximum at 10 m of the past bacterial and especially the archaeal biomass correspond to high HI values, indicating a higher aliphatic character of the OM and, therefore, maybe a better OM quality (Figs. 3 and 4b).

Additionally, while archaeol is basically derived from all archaeal kingdoms [*Koga and Morii,* 2007; *Schouten et al.,* 2013], crenarchaeol is suggested to be derived predominantly from Thaumarchaeota (archaeal kingdom) [*Leininger et al.,* 2006; *Schouten et al.,* 2013]. According to *Pitcher et al.* [2010], crenarchaeol could be a biomarker for ammonium-oxidizing Thaumarchaeota, which have already been identified in various soils and in Arctic environments [*Leininger et al.,* 2006]. Therefore, the shift in the archaeol/crenarchaeol ratio below 11.2 m not only reflects environmental changes but also indicate changes in the archaeal community [*Bischoff et al.,* 2013].

In general, interstadial periods in north Siberia are characterized by relatively high TOC, HI and TOC/TN and relative low $\delta^{13}C$, reflecting accumulation of less decomposed OM under wet and anaerobic soil conditions [*Wilkes et al.,* 1999; *Schirrmeister et al.,* 2011]. In addition to the TOC content and the available substrates, anoxic micro-habitats within water-filled soil pores are an important factor for the abundance of br-GDGTs containing bacteria in soils [*Weijers et al.,* 2006b]. Thus, the intervals of increased br-GDGT, iso-GDGT and archaeol concentrations in the Late Glacial/Early Holocene and Late Pleistocene deposits from Buor Khaya reveal time intervals of higher OM accumulation in presumably moister and maybe also warmer environments. A slight increase in permafrost temperature has not only an influence on the moisture content but also on the presence and diversity of the archaeal community, which can lead to a substantial increase of methanogenic activity [*Wagner et al.,* 2007]. Overall, periods of relatively increased temperatures during the Late Pleistocene caused tundra environments with water-saturated active layers [*Meyer et al.,* 2002; *Hubberten et al.,* 2004], forming excellent living conditions for br-GDGT containing bacteria [*Weijers et al.,* 2006a]. Additionally, the observed higher TOC contents in permafrost deposits mirror lower decomposition rates of the OM, which are characteristic for anaerobic conditions in water-saturated active layers [*Wetterich et al.,* 2014] likely caused by local hydrological changes and changes in local landscape dynamics (e.g. polygon dynamics) [*de Klerk et al.,* 2011].

5.3 Organic matter characteristics and microbial substrate potential for greenhouse gas production

The source of the OM is a controlling factor for its quality [*Meyers,* 1994]. The Larter-diagram (Fig. 4a) indicates terrestrial organic material (type III kerogen) with high phenol content deriving from lignin precursor species. The OI values, describing the amount of CO_2 produced during Rock-Eval pyrolysis normalized to the TOC content and indicating the proportions of oxygen-rich OM, also points to OM derived from terrestrial plant material. The low variability with depth might represent a constant proportion of terrestrial OM in the deposits with a slight increase with depth. The low OI value in the active layer and at 10 m depth is most likely related to the high aliphatic character of the OM as indicated by the HI values.

Depth intervals with increased organic carbon content (higher TOC) and quality (higher HI) show a higher aliphatic proportion (Fig. 4b), which might have derived from aliphatic rich terrestrial geopolymers such as cutin a polymer from waxy plant cuticles [*Kolattukudy,* 1980]. Another origin might be algae material from algae living in surface ponds. The lower $\delta^{13}C$ signal (Fig. 3e) of the 10 m sample with the high HI (Fig. 3b) might indicate that the stronger aliphatic character (Fig. 4b) is based on a significant contribution of waxy plant material.

Other source indicators are the ratio of TOC/TN, $\delta^{13}C$ values and the branched and isoprenoid tetraether (BIT) index. The TOC/TN values in the deposits are typical for the terrestrial permafrost deposits in this area [*Schirrmeister et al.,* 2011]. Following *Schirrmeister et al.* [2011], a small rise of the TOC/TN ratio (between 11.2 and 16.8 m) might resemble less degraded OM accumulated under wet and anaerobic soil conditions. Furthermore, the $\delta^{13}C$ values state an overall terrestrial, non-marine origin of the OM and mainly represent an increasing trend with depth, indicating a gradual increase in OM degradation. Additionally, the BIT index (see Table S1) based on the relative abundance of br-GDGTs, representing terrestrial OM, and crenarchaeol as indicator for aquatic OM

indicates the predominance of terrestrial microbial biomass [*Hopmans et al.,* 2004]. Only the samples below 15 m show lower BIT indices. Here, a different depositional environment is indicated also by lower TOC and decreased OM quality and a strong increase in sulfate concentration (Fig. 3h). However, since the BIT index is based on microbial markers it does only provide restricted information on origin of the OM.

An additional way to assess the quality of the OM with regard to its degradability is the investigation of potential substrates for microbial degradation. For instance, acetate is an excellent substrate for microbial turnover [*Ivarson and Stevenson,* 1964; *Sørensen and Paul,* 1971; *Sansone and Martens,* 1981; *Balba and Nedwell,* 1982] and a terminal electron acceptor for methanogens, especially in cold-temperate environments [*Chin and Conrad,* 1995; *Wagner and Pfeiffer,* 1997]. Methanogenic archaea are ubiquitous in anoxic environments and in permafrost sediments [*Kobabe et al.,* 2004]. Primarily, representatives of the genera Methanosarcina and Methanosaeta are able to use acetate as substrate for methanogenesis in permafrost-affected soils [*Ganzert et al.,* 2007]. Therefore, we use the acetate concentrations as an indicator for the quality of the OM with regard to microbial degradation and to assess the potential of the OM as a substrate provider for the production of the greenhouse gas methane.

Pore-water acetate represents an easily accessible substrate source for microbial metabolism, while the OM bound acetate forms a future substrate source upon release from the complex organic matrix structure by biotic and abiotic processes [*Glombitza et al.,* 2009]. The concentration of the bound acetate corresponds very closely to the TOC content. As discussed in the life marker chapter (5.1), the low abundance of free acetate in the active layer in contrast to the bound fraction is the result of high microbial acetate consumption by the active microbial communities during anaerobic decomposition (methanogenesis) [*Wagner et al.,* 2005]. In the active layer, highly specialized microorganisms such as methanogenic archaea and methane oxidizing bacteria are carrying out key processes of the methane cycle (*Kobabe et al.,* 2004; *Liebner and Wagner,* 2007; *Wagner et al.,* 2007). In reverse, the partly high acetate concentrations in the deeper permafrost sequence (interval III) revealing less microbial activity. For the interval I permafrost deposits and the interval III deposits between 11.2 and 15 m both the free and bound acetate pools suggest a high substrate potential of the deposited organic material for microbial turnover, in case this OM becomes bioavailable again due to deeper future permafrost thawing.

Nitrate is an important electron acceptor for a large group of heterotrophic facultative anaerobic bacteria to produce molecular nitrogen through a series of nitrogen products (denitrification) as part of the nitrogen cycle [*Jetten,* 2008]. In the active layer nitrate concentration is low also pointing to a high microbial activity in the surface layer (Fig. 3i). In contrast, higher nitrate concentrations occur in the permafrost sequence, which also will become bioavailable with future thawing. According to *Bodelier and Steenbergh* [2014] and *Koyama et al.* [2014], the nitrogen cycle and carbon cycle are strongly linked in permafrost soils and affected by permafrost thawing. Sulfate is another electron acceptor for specific anaerobic bacteria and archaea [*Hao et al.,* 1996]. Especially in the lowermost 2 m (Fig. 3h) of the core, the concentration of solved sulfate is strongly increased forming a significant electron acceptor pool for sulfate-reducing bacteria. Generally, sulfate-reducing bacteria are considered to play an important role in the anaerobic oxidation of methane [*Barton and Tomei,* 1995].

In the current study TOC, HI and the acetate concentrations are used as tracers to assess the quality of the deposited OM with respect to microbial degradability. In a scenario of ongoing permafrost thawing the data suggests that intervals of high organic carbon

contents during the Late Glacial/Early Holocene and Late Pleistocene sequences contain a high potential to act as a substrate provider for microbial degradation.

6 Conclusions

Abundant and active microbial life is indicated in the active layer of the Buor Khaya deposits. In contrast, microbial life is significantly lower and less active in the underlying permafrost deposits. Increased past microbial life within the permafrost sequence is linked to periods of higher terrestrial OM accumulation, often showing an increased aliphatic character. These organic-rich intervals might reflect formation under moister and warmer environmental conditions during the Late Pleistocene which causes shallow anaerobic soil conditions favorable for methanogenic communities. Thus, differences in the quality and amount of the OM in the Buor Khaya permafrost deposits seem to reflect past changes in the hydrology and local depositional environment.

The permafrost intervals with high OM accumulation are rich in potential substrates for methanogenesis. Thus, with regard to the generation of the greenhouse gas methane the OM freeze-locked in the permafrost deposits appears to be not much different in terms of OM quality than the younger surface organic material from the active layer. Therefore, the future potential for greenhouse gas generation from permafrost deposits seems to depend on the quality and amount of the stored OM rather than on the age. As a result of increased rates of deeper permafrost thaw in a warming Arctic, the observed similarities imply a significant impact on future generation of greenhouse gases from thawing permafrost areas with comparable OM deposits, including a positive feedback on climate evolution.

References

Anisimov, O. A. (2007), Potential feedback of thawing permafrost to the global climate system through methane emission, Environmental Research Letters, 2(4), 045016, doi:10.1088/1748-9326/2/4/045016.

Arkhangelov, A., D. Mikhalev, and V. Nikolaev (1996), Reconstruction of formation conditions of permafrost and climates in Northern Eurasia, History of permafrost regions and periglacial zones of Northern Eurasia and conditions of old human settlement"(AA Velichko, AA Arkhangelov, OK Borisova, et al., Eds.), 85-109.

Balba, M. T., and D. B. Nedwell (1982), Microbial metabolism of acetate, propionate and butyrate in anoxic sediment from Colne Point Saltmarsch, Essex, U.K., Journal of General Microbiology, 128 (7), 1415-1422, doi:10.1099/00221287-128-7-1415.

Barton, L. L., and F. A. Tomei (1995), Characteristics and activities of sulfate-reducing bacteria, in Sulfate-reducing bacteria, pp. 1-32, Springer US.

Bischoff, J., K. Mangelsdorf, A. Gattinger, M. Schloter, A. N. Kurchatova, U. Herzschuh, and D. Wagner (2013), Response of methanogenic archaea to Late Pleistocene and Holocene climate changes in the Siberian Arctic, Global Biogeochemical Cycles, 27(2), 305-317, doi:10.1029/2011GB004238.

Bligh, E. G., and W. J. Dyer (1959), A rapid method of total lipid extraction and purification, Canadian Journal of Biochemistry and Physiology, 37(8), 911-917, doi:10.1139/o59-099.

Bodelier, P. L., and A. K. Steenbergh (2014), Interactions between methane and the nitrogen cycle in light of climate change, Current Opinion in Environmental Sustainability, 9, 26-36, doi:10.1016/j.cosust.2014.07.004.

Chin, K.-J., and R. Conrad (1995), Intermediary metabolism in methanogenic paddy soil and the influence of temperature, FEMS Microbiology Ecology, 18(2), 85-102, doi:10.1111/j.1574-6941.1995.tb00166.x.

Christensen, T. R., T. Johansson, H. J. Akerman, M. Mastepanov, N. Malmer, T. Friborg, P. Crill, and B. H. Svensson (2004), Thawing sub-arctic permafrost: effects on vegetation and methane emissions, Geophysical Research Letters, 31(4), doi:10.1029/2003GL018680.

de Klerk, P., N. Donner, N. S. Karpov, M. Minke, and H. Joosten (2011), Short-term dynamics of a low-centred ice-wedge polygon near Chokurdakh (NE Yakutia, NE Siberia) and climate change during the last ca 1250 years, Quaternary Science Reviews, 30(21), 3013-3031, doi:10.1016/j.quascirev.2011.06.016.

Drozdov, D. S., F. M. Rivkin, V. Rachold, G. V. Ananjeva-Malkova, N. V. Ivanova, I. V. Chehina, M. M. Koreisha, Y. V. Korostelev, and E. S. Melnikov (2005), Electronic atlas of the Russian Arctic coastal zone, Geo-Marine Letters, 25(2-3), 81-88, doi:10.1007/s00367-004-0189-7.

Ganzert, L., G. Jurgens, U. Munster, and D. Wagner (2007), Methanogenic communities in permafrost-affected soils of the Laptev Sea coast, Siberian Arctic, characterized by 16S rRNA gene fingerprints, FEMS Microbiology Ecology, 59(2), 476-488, doi:10.1111/j.1574-6941.2006.00205.x.

Gilichinsky, D., and S. Wagener (1995), Microbial life in permafrost: a historical review, Permafrost and Periglacial Processes, 6(3), 243-250, doi:10.1002/ppp.3430060305.

Glombitza, C., K. Mangelsdorf, and B. Horsfield (2009), A novel procedure to detect low molecular weight compounds released by alkaline ester cleavage from low maturity coals to assess its feedstock potential for deep microbial life, Organic Geochemistry, 40(2), 175-183, doi:10.1016/j.orggeochem.2008.11.003.

Grosse, G., V. Romanovsky, T. Jorgenson, K. W. Anthony, J. Brown, P. P. Overduin, and A. Wegener (2011), Vulnerability and feedbacks of permafrost to climate change, EOS, Transactions, American Geophysical Union, 92(9), 73-74.

Günther, F., P. P. Overduin, A. S. Makarov, and M. Grigoriev (2013), Russian-German Cooperation SYSTEM LAPTEV SEA: The Expeditions Laptev Sea - Mamontov Klyk 2011 & Buor Khaya 2012, Berichte zur Polar-und Meeresforschung.

Günther, F., P. P. Overduin, I. A. Yakshina, T. Opel, A. V. Baranskaya, and M. N. Grigoriev (2015), Observing Muostakh disappear: permafrost thaw subsidence and erosion of a ground-ice-rich island in response to arctic summer warming and sea ice reduction, The Cryosphere, 9(1), 151-178, doi:10.5194/tc-9-151-2015.

Haack, S. K., H. Garchow, D. A. Odelson, L. J. Forney, and M. J. Klug (1994), Accuracy, reproducibility, and interpretation of fatty acid methyl ester profiles of model bacterial communities, Applied and Environmental Microbiology, 60(7), 2483-2493.

Hao, O. J., J. M. Chen, L. Huang, and R. L. Buglass (1996), Sulfate-reducing bacteria, Critical Reviews in Environmental Science and Technology, 26(2), 155-187, doi:10.1080/10643389609388489.

Hopkins, M. A. (1998), Four stages of pressure ridging, Journal of Geophysical Research: Oceans, 103(C10), 21883-21891, doi:10.1029/98JC01257.

Hopmans, E. C., J. W. H. Weijers, E. Schefuß, L. Herfort, J. S. Sinninghe Damsté, and S. Schouten (2004), A novel proxy for terrestrial organic matter in sediments based on branched and isoprenoid tetraether lipids, Earth and Planetary Science Letters, 224(1), 107-116, doi:10.1016/j.epsl.2004.05.012.

Horsfield, B., U. Disko, and F. Leistner (1989), The micro-scale simulation of maturation: outline of a new technique and its potential applications, Geologische Rundschau, 78(1), 361-373, doi:10.1007/BF01988370.

Hubberten, H. W., et al. (2004), The periglacial climate and environment in northern Eurasia during the Last Glaciation, Quaternary Science Reviews, 23(11), 1333-1357, doi:10.1016/j.quascirev.2003.12.012.

Hugelius, G., et al. (2014), Estimated stocks of circumpolar permafrost carbon with quantified uncertainty ranges and identified data gaps, Biogeosciences, 11(23), 6573-6593, doi:10.5194/bg-11-6573-2014.

Ivarson, K., and I. Stevenson (1964), The decomposition of radioactive acetate in soils: II. The distribution of radioactivity in soil organic fractions, Canadian Journal of Microbiology, 10(5), 677-682, doi:10.1139/m64-087.

Jetten, M. S. (2008), The microbial nitrogen cycle, Environmental Microbiology, 10(11), 2903-2909, doi:10.1111/j.1462-2920.2008.01786.x.

Knoblauch, C., C. Beer, A. Sosnin, D. Wagner, and E. M. Pfeiffer (2013), Predicting long-term carbon mineralization and trace gas production from thawing permafrost of Northeast Siberia, Global Change Biology, 19(4), 1160-1172, doi:10.1111/gcb.12116.

Kobabe, S., D. Wagner, and E. M. Pfeiffer (2004), Characterisation of microbial community composition of a Siberian tundra soil by fluorescence in situ hybridisation, FEMS Microbiology Ecology, 50(1), 13-23, doi:10.1016/j.femsec.2004.05.003.

Koga, Y., M. Nishihara, H. Morii, and M. Akagawa-Matshushita (1993), Ether polar lipids of methanogenic bacteria: structures, comparative aspects, and biosyntheses, Microbiological Reviews, 57(1), 164-182.

Koga, Y., and H. Morii (2006), Special methods for the analysis of ether lipid structure and metabolism in archaea, Analytical Biochemistry, 348(1), 1-14.

Koga, Y., and H. Morii (2007), Biosynthesis of ether-type polar lipids in archaea and evolutionary considerations, Microbiology and Molecular Biology Reviews, 71(1), 97-120, doi:10.1128/MMBR.00033-06.

Kolattukudy, P. E. (1980), Biopolyester membranes of plants: cutin and suberin, Science, 208, 990-1000, doi:10.1126/science.208.4447.990.

Koyama, A., M. D. Wallenstein, R. T. Simpson, and J. C. Moore (2014), Soil bacterial community composition altered by increased nutrient availability in Arctic tundra soils, Frontiers in Microbiology, 5, 516.

Larter, S. (1984), Application of analytical pyrolysis techniques to kerogen characterization and fossil fuel exploration/exploitation, in Analytical pyrolysis, edited, pp. 212-272, Butterworths London.

Lee, H., E. A. G. Schuur, K. S. Inglett, M. Lavoie, and J. P. Chanton (2012), The rate of permafrost carbon release under aerobic and anaerobic conditions and its potential effects on climate, Global Change Biology, 18(2), 515-527, doi:10.1111/j.1365-2486.2011.02519.x.

Leininger, S., T. Urich, M. Schloter, L. Schwark, J. Qi, G. W. Nicol, J. I. Prosser, S. C. Schuster, and C. Schleper (2006), Archaea predominate among ammonia-oxidizing prokaryotes in soils, NATURE, 442(7104), 806-809, doi:10.1038/nature04983.

Liebner, S., and D. Wagner (2007), Abundance, distribution and potential activity of methane oxidizing bacteria in permafrost soils from the Lena Delta, Siberia, Environmental microbiology, 9(1), 107-117, doi: 10.1111/j.1462-2920.2006.01120.x.

Lim, K. L., R. D. Pancost, E. R. Hornibrook, P. J. Maxfield, and R. P. Evershed (2012), Archaeol: an indicator of methanogenesis in water-saturated soils, Archaea, 2012, doi:10.1155/2012/896727.

Meyers, P. A. (1994), Preservation of elemental and isotopic source identification of sedimentary organic matter, Chemical Geology, 114(289-302), doi:10.1016/0009-2541(94)90059-0.

Meyer, H., A. Dereviagin, C. Siegert, L. Schirrmeister, and H.-W. Hubberten (2002), Palaeoclimate reconstruction on Big Lyakhovsky Island, north Siberia-hydrogen and oxygen isotopes in ice wedges, Permafrost and Periglacial Processes, 13(2), 91-105, doi:10.1002/ppp.416.

Müller, K. D., E. N. Schmid, and R. M. Kroppenstedt (1998), Improved identification of mycobateria by using the microbial identification system in combination with additional trimethylsulfonium hydroxide pyrolysis, Journal of Clinical Microbiology, 36(9), 2477-2480.

Pancost, R. D., J. S. Sinninghe Damste, S. de Lint, M. J. E. C. van der Maarel, and J. C. Gottschal (2000), Biomarker evidence for widespread anaerobic methane oxidation in Mediterranean sediments by a consortium of methanogenic Archaea and Bacteria, Applied and Environmental Microbiology, 66(3), 1126-1132, doi:10.1128/AEM.66.3.1126-1132.2000.

Pancost, R. D., E. C. Hopmans, and J. S. Sinninghe Damste (2001), Archaeal lipids in Mediterranean cold seeps: molecular proxies for anaerobic methane oxidation, Geochimica et Cosmochimica Acta, 65(10), 1611-1627, doi:10.1016/S0016-7037(00)00562-7.

Pancost, R. D., and J. S. Sinninghe Damsté (2003), Carbon isotopic compositions of prokaryotic lipids as tracers of carbon cycling in diverse settings, Chemical Geology, 195(1-4), 29-58, doi:10.1016/S0009-2541(02)00387-x.

Pancost, R. D., E. L. McClymont, E. M. Bingham, Z. Roberts, D. J. Charman, E. R. C. Hornibrook, A. Blundell, F. M. Chambers, K. L. H. Lim, and R. P. Evershed (2011), Archaeol as a methanogen biomarker in ombrotrophic bogs, Organic Geochemistry, 42(10), 1279-1287, doi:10.1016/j.orggeochem.2011.07.003.

Pease, T. K., E. S. Van Vleet, J. S. Barre, and H. D. Dickins (1998), Simulated degradation of glyceryl rthers by hydrous and flash pyrolysis, Organic Geochemistry, 29(4), 979-988, doi:10.1016/S0146-6380(98)00047-3.

Peters, K.E., C.C. Walters, and J.M Moldowan (2005), The Biomarker Guide (Vol. 1), Cambridge University Press

Pitcher, A., N. Rychlik, E. C. Hopmans, E. Spieck, W. I. Rijpstra, J. Ossebaar, S. Schouten, M. Wagner, and J. S. Damste (2010), Crenarchaeol dominates the membrane lipids of Candidatus Nitrososphaera gargensis, a thermophilic group I.1b Archaeon, The ISME Journal, 4(4), 542-552, doi:10.1038/ismej.2009.138.

Radke, M., H. Willsch, and D. H. Welte (1980), Preparative hydrocarbon group type determination by automated medium pressure liquid chromatography, Analytical Chemistry, 52(3), 406-411, doi:10.1021/ac50053a009.

Rilfords, L., A. Wieslander, and S. Stahl (1978), Lipid and protein composition of membranes of bacillus megaterium variants in the temperature range 5 to 70 degrees C, Journal of Bacteriology, 135(3), 1043-1052.

Rivkina, E., K. Laurinavichius, J. McGrath, J. Tiedje, V. Shcherbakova, and D. Gilichinsky (2004), Microbial life in permafrost, Advances in Space Research, 33(8), 1215-1221, doi:10.1016/j.asr.2003.06.024.

Romanovskii, N. N., H. W. Hubberten, A. V. Gavrilov, V. E. Tumskoy, and A. L. Kholodov (2004), Permafrost of the east Siberian Arctic shelf and coastal lowlands, Quaternary Science Reviews, 23(11-13), 1359-1369, doi:10.1016/j.quascirev.2003.12.014.

Romanovsky, V. E., et al. (2010), Thermal state of permafrost in Russia, Permafrost and Periglacial Processes, 21(2), 136-155, doi:10.1002/ppp.683.

Russell, N. J. (1989), Functions of lipids: Structural roles and membrane functions, in: Mircobial Lipids 2, Academic Press, 279-365.

Rütters, H., H. Sass, H. Cypionka, and J. Rullkötter (2002a), Phospholipid analysis as a toll to study complex microbial communities in marine sediments, Journal of Mircobiological Methods, 48 (2), 149-160, doi:10.1016/S0167-7012(01)00319-0.

Rütters, H., H. Sass, H. Cypionka, and J. Rullkötter (2002b), Microbial communities in a Wadden Sea sediment core - clues from analyses of intact glyceride lipids, and released fatty acids, Organic Geochemistry, 33(7), 803-816, doi:10.1016/S0146-6380(02)00028-1.

Sansone, F. J., and C. S. Martens (1981), Methane production from acetate and associated methane fluxes from anoxic coastal sediments, Science, 211(4483), 707-709, doi:10.1126/science.211.4483.707.

Schirrmeister, L., G. Grosse, S. Wetterich, P. P. Overduin, J. Strauss, E. A. G. Schuur, and H.-W. Hubberten (2011), Fossil organic matter characteristics in permafrost deposits of the northeast Siberian Arctic, Journal of Geophysical Research, 116 (G2), doi:10.1029/2011JG001647.

Schirrmeister, L., D. Froese, V. Tumskoy, G. Grosse, and S. Wetterich (2013), Yedoma: Late Pleistocene Ice-Rich Syngenetic Permafrost of Beringia. In: Elias S.A. (ed.) the Encyclopedia of Quaternary Science, 2nd edition, 542-552, doi:10.1016/B978-0-444-53643-3.00106-0.

Schirrmeister, L., G. Schwamborn, P. Overduin, J. Strauss, M.C. Fuchs, M.N. Grigoriev, I. Yakshina, J. Rethemeyer, E. Dietze, and S. Wetterich (2016, under review), Yedoma Ice Complex of the Buor Khaya Peninsula (southern Laptev Sea), Biogeosciences Discussions, doi:10.5194/bg-20160-283

Schouten, S., C. Huguet, E. C. Hopmans, M. V. M. Kienhuis, and J. S. Sinninghe Damsté (2007), Analytical methodology for TEX86 paleothermometry by high-performance liquid chromatography/atmospheric pressure chemical ionization-mass spectrometry, Analytical Chemistry, 79 (7), 2940-2944, doi:10.1021/ac062339v

Schouten, S., E. C. Hopmans, and J. S. Sinninghe Damsté (2013), The organic geochemistry of glycerol dialkyl glycerol tetraether lipids: A review, Organic Geochemistry, 54, 19-61, doi:10.1016/j.orggeochem.2012.09.006.

Schön, G. (1999), Bakterien: die Welt der kleinsten Lebewesen, CH Beck, München

Schuur, E. A., J. G. Vogel, K. G. Crummer, H. Lee, J. O. Sickman, and T. E. Osterkamp (2009), The effect of permafrost thaw on old carbon release and net carbon exchange from tundra, NATURE, 459(7246), 556-559, doi:10.1038/nature08031.

Sørensen, J., D. Christensen, and B. B. Jørgensen (1981), Volatile fatty acids and hydrogen as substrates for sulfate-reducing bacteria in anaerobic marine sediment, Applied and Environmental Microbiology, 42(1), 5-11.

Sørensen, L. H., and E. Paul (1971), Transformation of acetate carbon into carbohydrate and amino acid metabolites during decomposition in soil, Soil Biology and Biochemistry, 3(3), 173-180, doi:10.1016/0038-0717(71)90012-5.

Steven, B., R. Leveille, W. H. Pollard, and L. G. Whyte (2006), Microbial ecology and biodiversity in permafrost, Extremophiles, 10(4), 259-267, doi:10.1007/s00792-006-0506-3.

Strauss, J., L. Schirrmeister, S. Wetterich, and K. Mangelsdorf (2012), Old Organic Matter in Siberian Permafrost Deposits and its Degradation Features, Tenth International Conference on Permafrost, Salekhard, Russia.

Strauss, J., L. Schirrmeister, K. Mangelsdorf, L. Eichhorn, S. Wetterich, and U. Herzschuh (2015), Organic-matter quality of deep permafrost carbon – a study from Arctic Siberia, Biogeosciences, 12(7), 2227-2245, doi:10.5194/bg-12-2227-2015.

Talbot, M. R., and D. A. Livingstone (1989), Hydrogen index and carbon isotopes of lacustrine organic matter as lake level indicators, Palaeogeography, Palaeoclimatology, Palaeoecology, 70 (1), 121-137, doi:10.1016/0031-0182(89)90084-9.

Vieth, A., K. Mangelsdorf, R. Sykes, and B. Horsfield (2008), Water extraction of coals – potential for estimating low molecular weight organic acids as carbon feedstock for the deep terrestrial biosphere, Organic Geochemistry, 39(8), 985-991, doi:10.1016/j.orggeochem.2008.02.012.

Wagner, D., and E.-M. Pfeiffer (1997), Two temperature optima of methane production in a typical soil of the Elbe river marshland, FEMS Microbiology Ecology, 22(2), 145-153, doi:10.1111/j.1574-6941.1997.tb00366.x.

Wagner, D., S. Kobabe, E. M. Pfeiffer, and H. W. Hubberten (2003), Microbial controls on methane fluxes from a polygonal tundra of the Lena Delta, Siberia, Permafrost and Periglacial Processes, 14(2), 173-185, doi:10.1002/ppp.443.

Wagner, D., A. Lipski, A. Embacher, and A. Gattinger (2005), Methane fluxes in permafrost habitats of the Lena Delta: effects of microbial community structure and organic matter quality, Environmental microbiology, 7(10), 1582-1592, doi:10.1111/j.1462-2920.2005.00849.x.

Wagner, D., A. Gattinger, A. Embacher, E.-M. Pfeiffer, M. Schloter, and A. Lipski (2007), Methanogenic activity and biomass in Holocene permafrost deposits of the Lena Delta, Siberian Arctic and its implication for the global methane budget, Global Change Biology, 13(5), 1089-1099, doi:10.1111/j.1365-2486.2007.01331.x.

Washburn, A. L. (1980), Permafrost features as evidence of climatic change, Earth-Science Reviews, 15(4), 327-402, doi:10.1016/0012-8252(80)90114-2.

Weijers, J. W., S. Schouten, E. C. Hopmans, J. A. Geenevasen, O. R. David, J. M. Coleman, R. D. Pancost, and J. S. Sinninghe Damste (2006a), Membrane lipids of mesophilic anaerobic bacteria thriving in peats have typical archaeal traits, Environmental Microbiology, 8(4), 648-657, doi:10.1111/j.1462-2920.2005.00941.x.

Weijers, J. W. H., S. Schouten, O. C. Spaargaren, and J. S. Sinninghe Damsté (2006b), Occurrence and distribution of tetraether membrane lipids in soils: Implications for the use of the TEX86 proxy and the BIT index, Organic Geochemistry, 37(12), 1680-1693, doi:10.1016/j.orggeochem.2006.07.018.

Wetterich, S., N. Rudaya, V. Tumskoy, A. A. Andreev, T. Opel, L. Schirrmeister, and H. Meyer (2011a), Last Glacial Maximum records in permafrost of the East Siberian Arctic, Quaternary Science Reviews, 30(21), 3139-3151, doi:10.1016/j.quascirev.2011.07.020.

Wetterich, S., P. P. Overduin, and M. Grigoriev (2011b), Russian-German Coopration SYSTEM LAPTEV SEA: The expedition Eastern Laptev Sea - Buor Khaya Peninsula 2010, Berichte zur Polar-und Meeresforschung.

Wetterich, S., V. Tumskoy, N. Rudaya, A. A. Andreev, T. Opel, H. Meyer, L. Schirrmeister, and M. Hüls (2014), Ice Complex formation in arctic East Siberia during the MIS3

Interstadial, Quaternary Science Reviews, 84, 39-55, doi:10.1016/j.quascirev.2013.11.009.

White, D. C., W. M. Davis, J. S. Nickels, J. D. King, and R. J. Bobbie (1979), Determination of the sedimentary microbial biomass by extractible lipid phosphate, Oecologia, 40(1), 51-62, doi:10.1007/BF00388810.

Wilkes, H., A. Ramrath, and J. F. Negendank (1999), Organic geochemical evidence for environmental changes since 34,000 yrs BP from Lago di Mezzano, central Italy, Journal of Paleolimnology, 22(4), 349-365, doi:10.1023/A:1008051821898.

Zelles, L. (1999), Fatty acid patterns of phospholipids and lipopolysaccharides in the characterisation of microbial communities in soil: a review, Biology Fertility of Soils, 29(2), 111-129, doi:10.1007/s003740050533.

Zimov, S. A., S. P. Davydov, G. M. Zimova, A. I. Davydova, E. A. G. Schuur, K. Dutta, and F. S. Chapin (2006), Permafrost carbon: Stock and decomposability of a globally significant carbon pool, Geophysical Research Letters, 33(20), doi:10.1029/2006GL027484.

Zink, K. G., H. Wilkes, U. Disko, M. Elvert, and B. Horsfield (2003), Intact phospholipids-microbial "life markers" in marine deep subsurface sediments, Organic Geochemistry, 34(6), 755-769, doi:10.1016/S0146-6380(03)00041-x.

Zink, K. G., and K. Mangelsdorf (2004), Efficient and rapid method for extraction of intact phospholipids from sediments combined with molecular structure elucidation using LC-ESI-MS-MS analysis, Analytical and Bioanalytical Chemistry, 380(5), 798-812, doi:10.1007/s00216-004-2828-2.
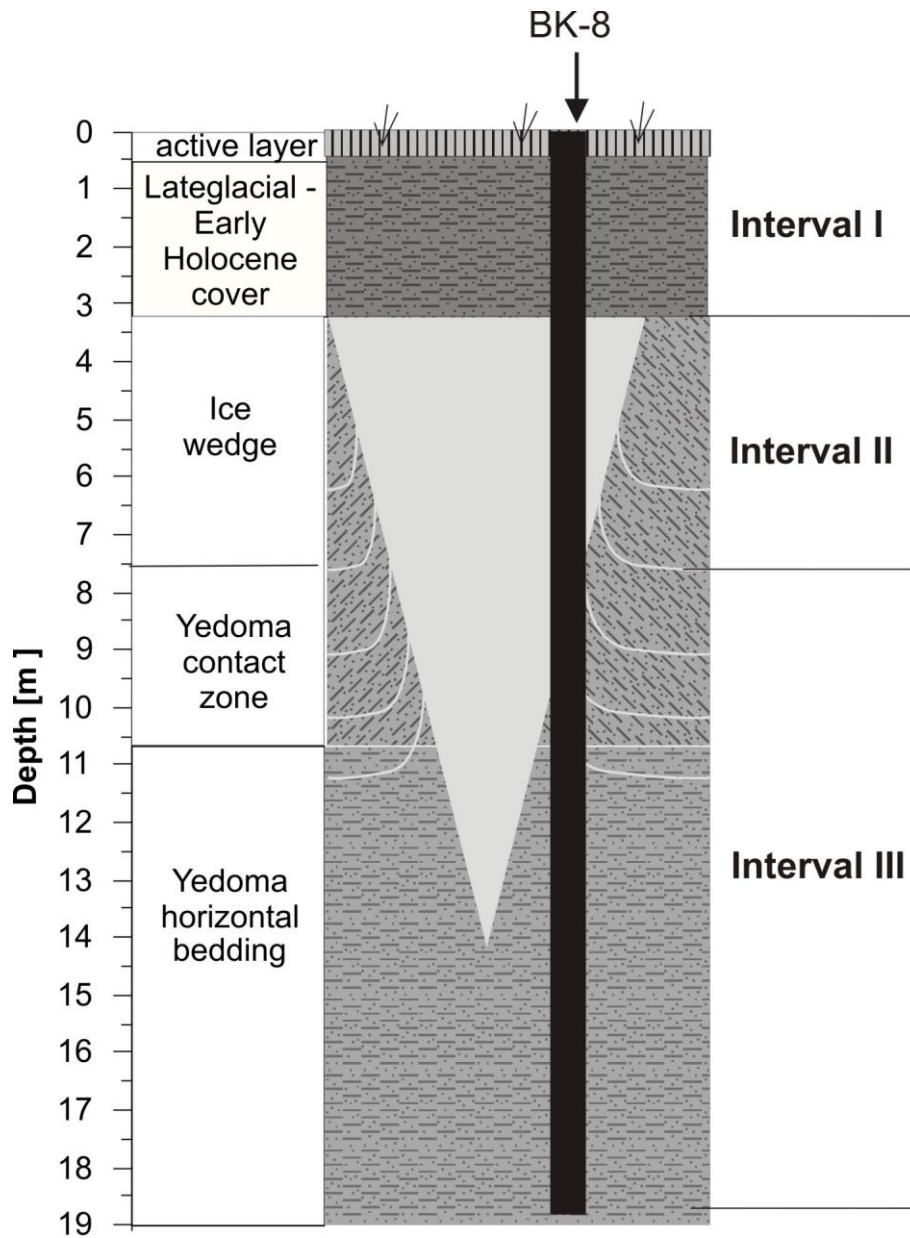
Figure 1. Position of the Buor Khaya Peninsula in the Siberian Arctic (a). Buor Khaya Peninsula study site in northeastern Siberia (b), and location of the drill site (BK-8), marked with black star (c).
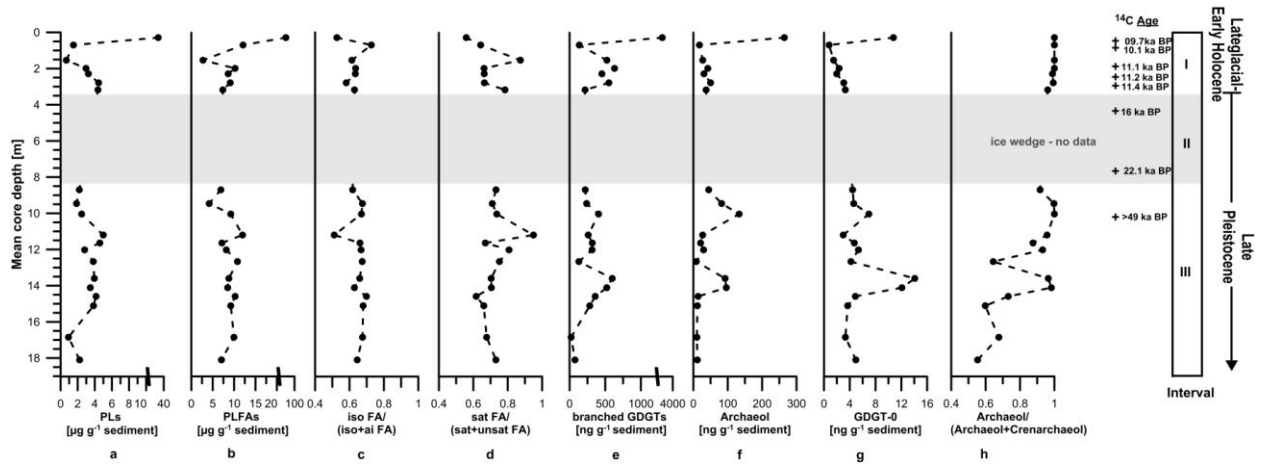
Figure 2. BK-8 stratigraphical scheme modified according to *Schirrmeister et al.,* [2016] including interval classification.
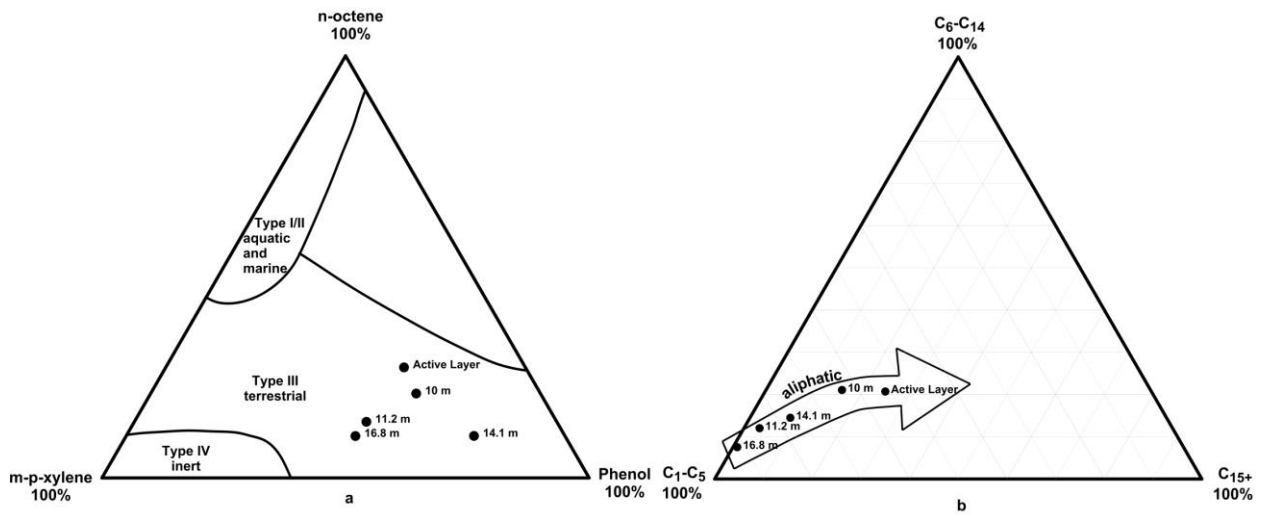
Figure 3. Geochemical parameters of the permafrost core from the Buor Khaya peninsula, Siberia, presented with respect to core depth (left axis) and sediment age [*Schirrmeister et al.,* 2016] (right column). The vertical profiles show: a. the TOC content in wt%; b. the ratio of total organic carbon and total nitrogen (TOC/TN); c. the hydrogen index in mg HC/gTOC; d. the oxygen index in mg CO_2/gTOC; e. the $\delta^{13}C_{org}$ in ‰; f. the concentration of free acetate in mg/l; g. concentration of bound acetate in mg/1; h. concentration of sulfate in mg/l; i. concentration of nitrate in mg/l.
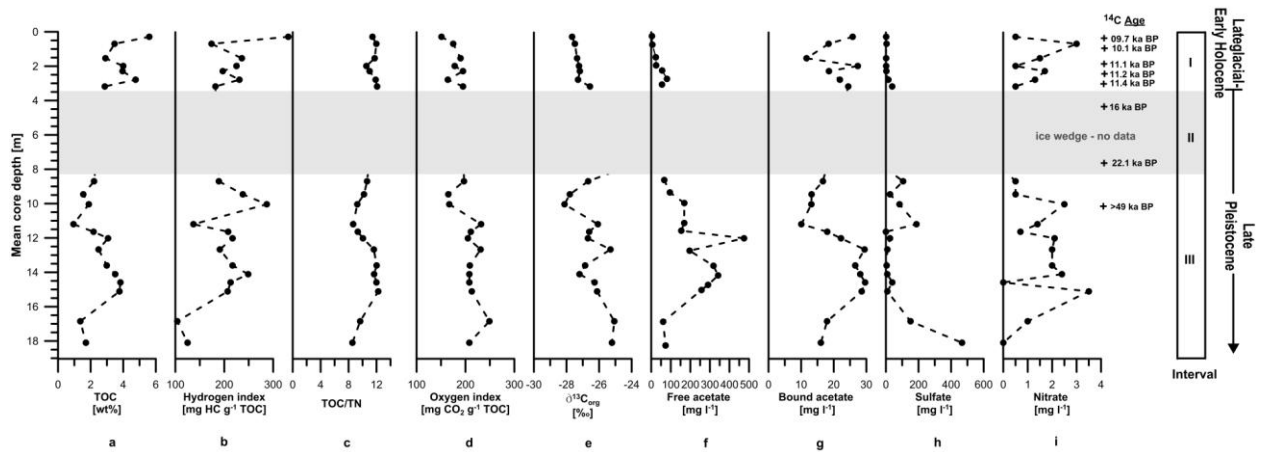
Figure 4. Triangular plots derived from organic matter pyrolysis. (a) Larter-diagram: Classification of the kerogen type (type I/II: aquatic and marine; type III: terrestrial; type IV: inert organic material) due to the relative abundance of meta-, para-xylene (*m,p*-xylene), *n*-octene and phenol in the organic matter after *Larter* [1984]. (b) Horsfield-diagram: Composition of the organic matter according to the chain length distribution of short (C_1-C_5), intermedia (C_6-C_{14}) and long (C_{15+}) *n*-alk-1-enes plus *n*-alkanes after *Horsfield et al.* [1989]. The arrow indicates an increasing aliphatic proportion in the organic matter of the investigated samples.
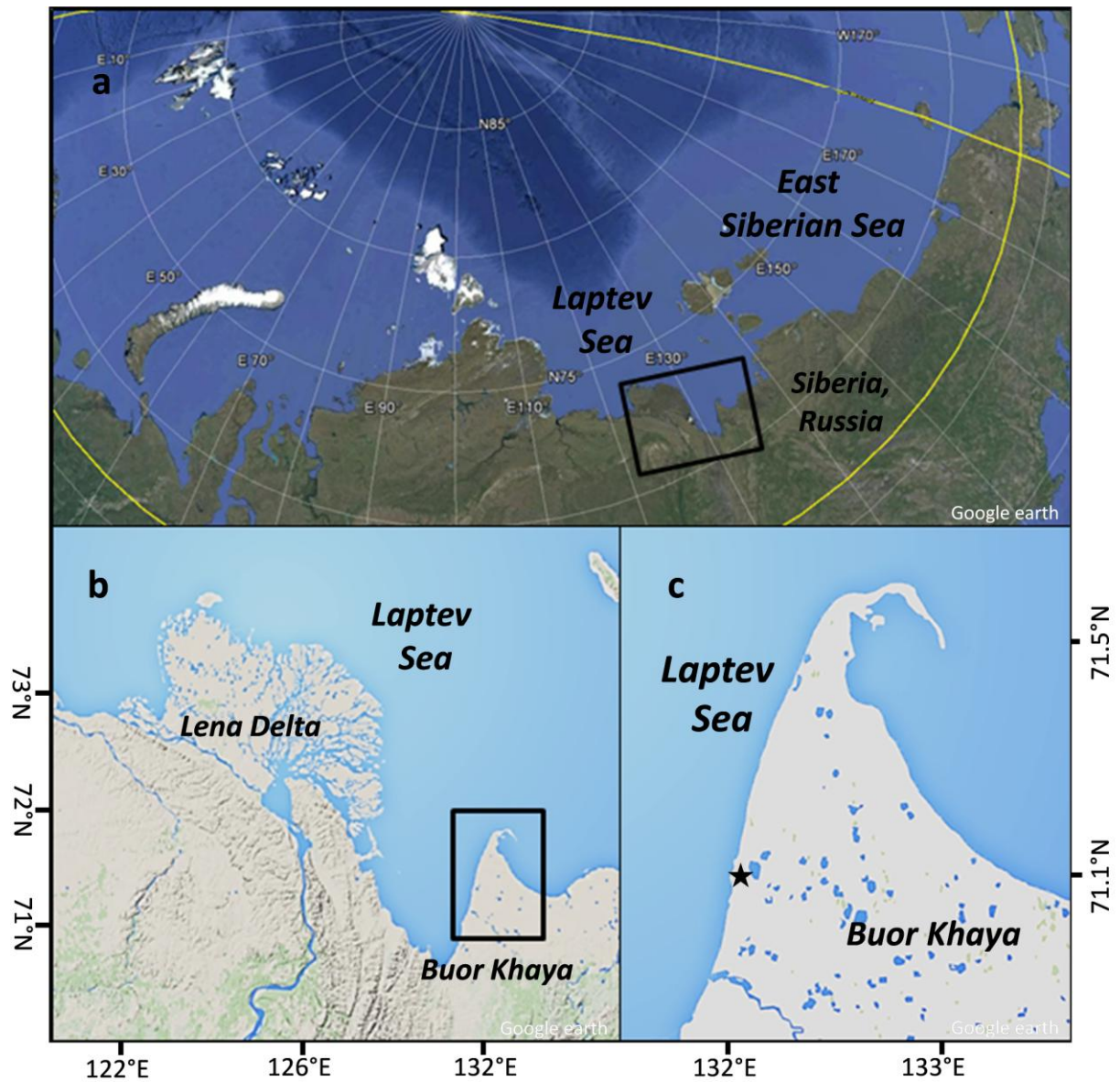
Figure 5. Microbial biomarker parameters of the permafrost core from the Buor Khaya peninsula, Siberia, presented with respect to core depth (left axis) and sediment age [*Schirrmeister et al.,* 2016] (right column). The vertical profiles show: a. concentration of phospholipids (PLs) in µg/gSed.; b. concentration of phospholipid fatty acids (PLFAs) in µg/gSed.; c. ratio of *iso-* and *anteiso*-fatty acids (FA); d. ratio of saturated and unsaturated FA; e. the concentration of branched glycerol dialkyl glycerol tetraethers (GDGTs) in ng/gSed.; f. the concentration of archaeol in ng/gSed; g. the concentration of glycerol dibiphytanyl glycerol tetraether (GDGT-0) in ng/gSed; h. the ratio of archaeol and crenarchaeol.